International Journal of Mechanical, Industrial and Aerospace Sciences
ISSN: 2517-9950
Vol:12, No:7, 2018

Modeling of the Cavitation by Bubble around a NACA0009 Profile

L. Hammadi, D. Boukhaloua

Abstract**—**In this study, a numerical model was developed to predict cavitation phenomena around a NACA0009 profile. The equations of the Rayleigh-Plesset and modified Rayleigh-Plesset are used to modeling the cavitation by bubble around a NACA0009 profile. The study shows that the distributions of pressures around extrados and intrados of profile for angle of incidence equal zero are the same. The study also shows that the increase in the angle of incidence makes it possible to differentiate the pressures on the intrados and the extrados.

Keywords**—**Cavitation, NACA0009 profile, flow, pressure coefficient.

I. Introduction

THE cavitation remains, today, a major concern for those interested in the design and operation of many industrial components such as: turbines, pumps, thrusters, cryogenic engines, valves, etc. The phenomenon of cavitation is characterized by the formation of vapor bubbles in its liquid in a strong depression [1]. According to Maiga and Buisine [2], the high depression is the origin of the cavitation, and its appearance is influenced by several factors, including micro-gaseous inclusions called germs of cavitation. The damage due to cavitation has been studied by [3] thanks to the laser profilometry. It shows that the ratio between the pit radius and pit depth is not constant and it usually lies between 15 and 30, but it can also be as low as 2 and as high as 500.

A Rayleigh model for a single collapsing bubble with assumed toroidal shape including a harmonics analysis in relation to potential erosion caused by such a bubble was developed by Prikhodko et al. [4]. The authors demonstrated that the number of germs may depend on the nature of the fluid and the treatment that it has undergone. According to Ohl [5], the birth of cavitation bubbles of microscopic size may develop over time to give macroscopic vapor bubbles. Likewise, the author suggested that the cavitation bubbles becoming visible are formed from multiple stabilized gas pockets. The visualization of the evolution of the vapor bubble generated by the sparker, simultaneously acquiring the acoustic wave has been investigated by Buogo and Cameli [6]. The authors noted that the emission of sound during the evolution of cavitation micro-bubbles are continually produced and reabsorbed. The very early disappearance of small bubbles was thus highlighted by the authors as well as by [7] which show that a light emission, signature of collapses, is observed from the beginning of cavitation. Many models are used for modeling the cavitation, including the germ model [8], the production/transport model of the vacuum rate [9], and the bubble model that attempts to model the microscopic state of cavitation. To take into account the influence of other cloud bubbles on the evolution of the main bubble, Wang and Ostoja-Starzewski [10] modified the Rayleigh equation by introducing the average growth rate of the other bubbles with the assumption that cloud bubbles all undergo the same expansion. In this study, we propose a new model of bubble to predict the cavitation phenomena in a hydraulic machine.

L. Hammadi is with the Laboratory of Rheology, Transport and Treatment of the Complex Fluids, University of Science and Technology, Mohamed Boudiaf, B.P. 1505, El M'Naour, Oran 31000, Algeria (e-mail: hammadi7280@yahoo.fr).

D. Boukhaloua is with the Department of English, University of Ahmed Ben Ahmed, Oran 2, Algeria (e-mail: hammadidjamila@hotmail.fr).

II. Modeling the Cavitation's by Bubble

A. Hypotheses

If one assumes a permanent and stable flow without vorticity and far from any wall, one can emit the following hypotheses [11], [12]:

- Bubbles are always spherical. Indeed, since it is only the beginning of cavitation that interests us, we can suppose that the bubbles remain small. Factors that can create spherical dis-symmetries have less influence on small bubbles than on large ones. These bubbles, having only a very short life, are not much solicited by the disturbances of their environment;
- The initiation of a bubble is made from a cavitation germ. The phase change is triggered when the critical pressure of a seed is reached;
- The microscopic flow around the bubble is incompressible, viscous, and irrational. It is assumed that near the outer radius of the bubble, the fluid moves only radially following the evolution of the radius of the bubble;
- The bubble is in equilibrium initially, and its internal pressure is the sum of the pressures of the vapor and gas.

We neglect mass transfers that may occur at the walls of the bubble. The transfers of the gases contained in the bubble occur with a time scale greater than that of the lifetime of the cavitation bubble. For vaporizing water, the mass volume of steam is about a thousand times larger than that of water, and the dynamics of the vapor will have a negligible effect on the dynamics of the water. An adiabatic evolution of the gases contained in the bubble is supposed. The determining factor is the ratio of the specific heats of the gas.

B. Modeling of Cavitation

To obtain the bubble model, we start from the continuity equation in spherical coordinates in a supposed incompressible liquid (Fig. 1), outside the bubble:

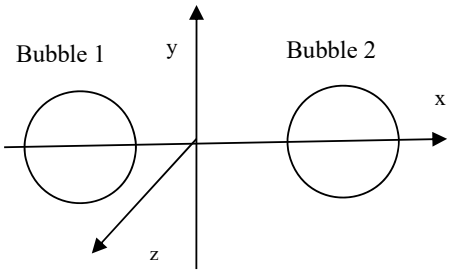

Fig. 1 Positioning two bubbles on their center line

The momentum equation takes the following form in spherical coordinates

$$\frac{\partial C_r}{\partial t} + C_r \frac{\partial C_r}{\partial t} = -\frac{1}{\rho}\frac{\partial P(t)}{\partial r} + \nu\left[\frac{1}{r^2}\frac{\partial}{\partial r}(r^2\frac{\partial C_r}{\partial t})\right] - 2\frac{C_r}{r^2} \quad (1)$$

where $C_r = \frac{R^2}{r^2}\frac{dR}{dt}$ is the velocity of the flow at the radius r, R is the radius of the bubble, p(t) is the pressure around the bubble.

By replacing C_r in (1) and integrating between 0 and R, we obtain

$$p(R) = P_\infty(t) + \rho\left[R\frac{d^2R}{dt^2} + \frac{3}{2}(\frac{dR}{dt})^2\right] \quad (2)$$

where p(R) is the pressure at the bubble interface of the liquid side and p_r pressure away from the wall of the bubble at $r \to \infty$.

The evolution of gases in the variable volume bubble is considered as adiabatic with the polytropic exponent λ. The momentum equation takes the following form in spherical coordinates:

$$p_g = p_{g0}\left[\frac{R_0}{R}\right]^{3\lambda} \quad (3)$$

with

$$p_{g0} = p(R_0) - p_v + \frac{2\gamma}{R_0} \quad (4)$$

The pressure balance between the inside peripheral and the outside peripheral of the bubble is given by:

$$p_g + p_V - \frac{2\gamma}{R_0} = p(R) + \frac{4\mu}{R}\frac{dR}{dt} \quad (5)$$

By grouping (4) and (3), we obtain the pressure p_g of the gases contained in the bubble, as a function of the radius of the bubble and its derivative:

$$p_g = \left[p_0 - p_v + \frac{2\gamma}{R_0}\right]\left[\frac{R_0}{R}\right]^{3\lambda} \quad (6)$$

Equation (6) is included in (5)

$$\left[p_0 - p_V + \frac{2\gamma}{R_0}\right]\left[\frac{R_0}{R}\right]^{3\lambda} + p_V - \frac{2\gamma}{R_0} = p(R) + \frac{4\mu}{R}\frac{dR}{dt} \quad (7)$$

Just replace p(R) with the result of (2) to get the RayLeigh-Plesset equation in its dimensional form

$$\rho\left[R\frac{d^2R}{dt^2} + \frac{3}{2}\left(\frac{dR}{dt}\right)^2 + \frac{4v}{R}\frac{dR}{dt}\right] = \left(p_v - p(t)\right) - \frac{2\gamma}{R}\left[\frac{2\gamma}{R_0} - (p_V - p_0)\right]\left(\frac{R_0}{R}\right)^{3\lambda} \quad (8)$$

This last equation can be put into the dimensionless form by dividing all the terms by the dynamic pressure of the flow $\frac{1}{2}\rho C_0^2$. We then find the Rayleigh-Plesset equation non-dimensional form:

$$2r\ddot{r} + 3\dot{r}^2 + \frac{8}{R_e}\frac{\dot{r}}{r} + \frac{4}{W_e^2}\frac{1}{r} - G\frac{1}{r^{3\lambda}} = -\sigma - C_p(t) \quad (9)$$

$r = \frac{R}{L}$, $\dot{r} = \frac{\dot{R}}{C_0}$, $\ddot{r} = \frac{L\ddot{R}}{C_0^2}$, $R_e = \frac{C_0 L}{\nu}$ Reynolds number, $W_e = \frac{C_0 L^{1/2}}{(\gamma/\rho)^{1/2}}$ Weber number, $\sigma = \frac{p_0 - p_V}{\frac{1}{2}\rho C_0^2}$ number of cavitation and $G = r^{3\lambda}\frac{4}{W_e^2}\frac{1}{r_0}$ a constant.

The coefficient of the driving pressure is given by:

$$C_p(t) = \frac{p(t) - p_0}{\frac{1}{2}\rho C_0^2} \quad (10)$$

With the use of a turbine in an industrial context, the following additional assumptions are made:

- the viscosity of the water is negligible during most of the evolution of the bubble;
- the germ radius is much smaller than that of the developed bubble;
- the contribution of the gases contained in the bubble and the effects of surface tension on the pressure in the bubble are negligible.

The Rayleigh-Plesset equation, in dimensional form, adapted to our problem then returns to the following form:

$$\rho R\frac{d^2R}{dt^2} + \frac{3\rho}{2}\left(\frac{dR}{dt}\right)^2 = p_V - p_\infty \quad (11)$$

Or, in form non-dimensional:

$$2r\ddot{r} + 3\dot{r} = -\sigma - C_p(t) \quad (12)$$

III. Results and Discussion

A. Rayleigh-Plesset and Integration of 4th Order Runge-Kutta

To obtain more precision, we calculate the radius of a vapor bubble and its displacement. We are tempted to use a numerical scheme for solving (9). The most used algorithm to solve a linear differential equation is that of Runge-Kutta. We note that the simplifications made to the original Rayleigh-Plasset (9) to obtain (12) are justified by the quasi-

superposition of the curves (Fig. 2). This simplification makes it possible to reduce the calculation time by a factor of two while not affecting the result. The latter will be the basis of the bubble model. The non-dimensional time scale is defined as the period of time from which a fluid particle passes the leading edge of the divided profile by the time required by the particle to traverse the entire extrados side of the profile.

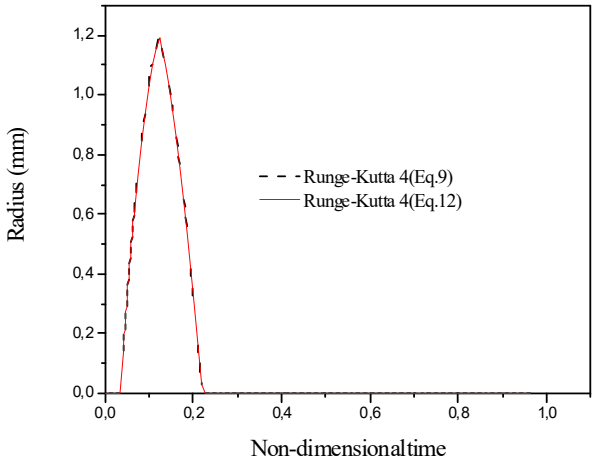

Fig. 2 Radius of bubble calculated on the extrados of the NACA0009 profile for an incidence of 0.5 degrees with σ = 0.38

B. Influence of Angle of Incidence on the Radius of the Bubble

Fig. 3 shows the variation of radius of the bubble (R) as a function of x/c for different angles of incidence. From the figure, it is noted that the increase in the angle of incidence causes an increase in radius of the bubble on the extrados of the profile and a development of a cavitation towards the leading edge of the profile.

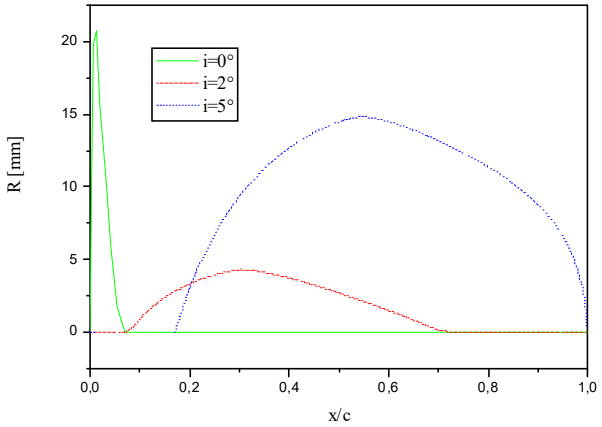

Fig. 3 Influence of angle of incidence on the radius of the bubble

C. Influence of Angle of Incidence on the Pressure Coefficient

Fig. 4 shows the variation of the pressure coefficient on the lower surface and upper surface of a symmetrical profile NACA 0009 as a function of the position on the profile, by varying the angle of incidence of the profile (the pressure coefficient is calculated by the panel method). Note that for a profile with zero incidence, the pressures are distributed in the same way on the intrados and extrados, which is normal (Fig. 5). On the walls of the profile, the tangential velocity is greater than the infinite velocity (velocity of air), because the streamlines of the fluid, considered perfect, are close to each other, which, by applying the conservation theorem of the flow, allows us to say that the speed along the profile is higher. Hence, by applying Bernoulli's theorem, we deduce that the pressure along this same profile is less than that at infinity. This phenomenon is particularly visible just after the leading edge. But, it is not verified at the level of the leading edge itself, which is a stopping point, so where the speed vanishes, and where the Cp tends to 1. One has likewise a deceleration at the edge. Leak that increases the Cp. The increase in the incidence makes it possible to differentiate the pressures on the intrados and the extrados. On the extrados, the tangential velocity increases with respect to the normal speed under zero angle of incidence, therefore the pressure decreases with respect to the zero-incidence profile.

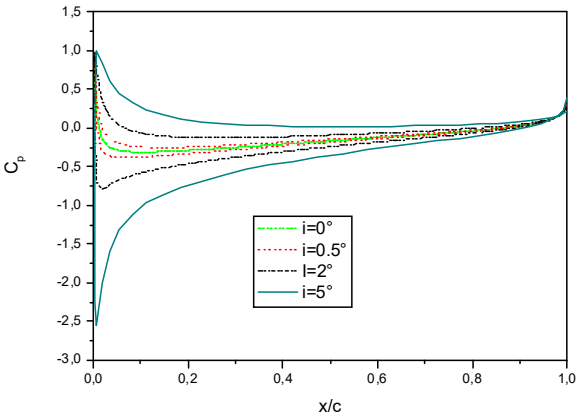

Fig. 4 Variation of the pressure coefficient (Cp) as a function of the angle of incidence on the extrados and the intrados of a NACA0009 profile

TABLE I
UNITS FOR CAVITATION MODELING

Symbol	Quantity	Conversion from Gaussian and CGS EMU to SI [a]
$C_p(t)$	coefficient of the driving pressure	-
C_r	velocity of the flow	m/s
r, R	radius	m
p(t)	pressure around the bubble	Pa
R_e	Reynolds number	-
W_e	Weber number	-
σ	number of cavitation	-
λ	polytropic exponent	-
i	angle of incidence	°

In contrast, the intrados sees its decreased tangential velocity compared to the previous one, because of the increase of the obstacle that produces the wing with the flow coming from the infinity. Hence, pressure increases compared to the

zero-incidence profile. The breakpoint is always the leading edge, so the pressure always tends to 1 at this level.

IV. Conclusion

During this study, a numerical model was developed in order to predict the phenomena of cavitation in a hydraulic machine. The bubble radius is calculated by the bubble model, moreover it is observed for our calculations that the maximum radius of the bubbles as well as their lifetimes are insensitive to the variations of initial radius of the germs, so the initial radius of the bubble has no effect on the radius of the bubble. The study showed the increase the angle of incidence caused an increase in the radius of the bubble on the extrados of the profile and a development of a cavitation towards the leading edge of the profile.

References

[1] W. Lauterborn, W. Hentschel, "Cavitation bubble dynamics studied by high speed photography and holography: part two," Ultrasonics, 1986, pp.59-69.
[2] M. AnamaMaiga, D. Buisine, "Modèle multi-bulles pour la cavitation," C.R Mécanique, 2009, pp.791-800.
[3] R. Fortes-Patella, J. Reboud, A. Archer "Cavitation damage measurement by 3D laser profilometry," Wear 2000, pp. 59-69.
[4] V. Prikhodko, A. Buslaev, M. Norkin, M. Yashina, "Modelling of cavitational erosion in the area of surfaces of smooth contact," Ultrasonics Sonochemistry, 2001, pp.59-67.
[5] D. Ohl, "Cavitation inception following shock wave passage," Phys. Fluids, 2002, pp.3512-3521.
[6] S. Buogo, G. Cameli, "Implosion of an underwater spak-generated and bubble and acoustic energy evaluation using the Rayleigh model," J. Acoust. sc. Am, 2002, pp.2594-2599.
[7] S. Takahashi, S. Washio, K. Uemura, A. Okazaki,"Experimental study on cavitation starting at and flow characteristics close to the point of separation," Fifth International Symposium on Cavitation, Osaka, Japan, November 2003, pp.1–4.
[8] J. Franc"La cavitation mécanisme physique et aspects industriels," Presses Universitaires de Grenoble 1995 France.
[9] M. Ishii, "Thermo-fluid dynamic theory of two-phase Flow," Collection de la direction des études et recherches d'électricité de France, Eyrolles, 1975.
[10] G. Wang, M. Ostoja-Starzewski, "Large eddy simulation of a sheet/cloud cavitation on a NACA0015 hydrofoil," Applied Mathematical Modelling, 2007, vol.31, pp.417-447.
[11] M. Cudina, "Detection of cavitation phenomenon in a centrifugal pump using audible sound,'' Mechanical System and Signal Processing, 2003, pp.1335–1347.
[12] C. E. Brennen. "Cavitation and Bubble Dynamics," Oxford University Press, Oxford, 1995.